
Prototype-based Neural Network Layers: Incorporating Vector Quantization

Sascha Saralajew

Dr. Ing. h.c. F. Porsche AG
Weissach, Germany
sascha.saralajew@porsche.de

Lars Holdijk

Dr. Ing. h.c. F. Porsche AG
Weissach, Germany
lars.holdijk@porsche.de

Maike Rees

Dr. Ing. h.c. F. Porsche AG
Weissach, Germany
maike.rees@porsche.de

Thomas Villmann

University of Applied Sciences Mittweida
Mittweida, Germany
thomas.villmann@hs-mittweida.de

Abstract

Neural networks currently dominate the machine learning community and they do so for good reasons. Their accuracy on complex tasks such as image classification is unrivaled at the moment and with recent improvements they are reasonably easy to train. Nevertheless, neural networks are lacking robustness and interpretability. Prototype-based vector quantization methods on the other hand are known for being robust and interpretable. For this reason, we propose techniques and strategies to merge both approaches. This contribution will particularly highlight the similarities between them and outline how to construct a prototype-based classification layer for multilayer networks. Additionally, we provide an alternative, prototype-based, approach to the classical convolution operation. Numerical results are not part of this report, instead the focus lays on establishing a strong theoretical framework. By publishing our framework and the respective theoretical considerations and justifications before finalizing our numerical experiments we hope to jumpstart the incorporation of prototype-based learning in neural networks and vice versa.

1 Introduction

Neural networks (NNs) are currently the state of the art for a wide range of complex machine learning problems like image classification or regression tasks. Empowered by hardware support as well as developments in normalization techniques [1], activation functions [2, 3] and new architectures [4, 5, 6], it is hard to ignore NNs. Another reason for their success is that they are often trained in an end-to-end manner. This means that there are no intermediate outputs but the network approximates a function that maps from the input directly to the output decision. The end-to-end approach however also comes with some disadvantages, such as making the network hard to interpret, especially in real time. This has led to a lot of hesitation in implementing NNs in safety critical systems, such as autonomous cars. This hesitation is further increased by their lack of robustness. A trained model can be vulnerable to adversarial attacks [7]. In an adversarial attack, the network is presented an input with a perturbation that is imperceptible for the human eye, causing the model to misclassify the input. Despite the recent efforts of the community and the progress made in the understanding of these pitfalls, even resulting in provable robustness guarantees [8], to this day even the best methods are not as robust as humans in classifying handwritten digits from the MNIST dataset [9].¹

¹Surprisingly, if we follow the results in [9], one of the most robust methods on MNIST is a simple k-nearest-neighbor classifier, which is a predecessor of Learning Vector Quantization.

Prototype-based vector quantization methods (PBs) are generally known for being interpretable, robust, sparse in the sense of memory complexity and fast to train and to evaluate. PBs rely on the concept of a distance/dissimilarity² measure for classification, giving the approach an inherent geometrically interpretable robustness. Despite PBs being proposed over 20 years ago, these algorithms, and particularly their recent improvements and extensions, are widely unknown or ignored by the current machine learning community. An exception are the quite simple and frequently impracticable k-means or k-nearest-neighbor algorithms. Drawbacks of PBs are that they frequently cannot compete with the accuracy of modern (deep) neural network architectures. If the task (data) is complex, like in image classification, the direct input of the image to the classification is not suitable and requires image features to be computed a-priori.

Our contribution in this technical report is to bridge the gap between NNs and PBs. Right now, both methods are treated as completely different, or even worse as competing or not compatible with each other. This technical report will show that this is not the case and that the methods are more related to each other than one might expect at the first glance. We will not present numerical results, but rather present a conceptual framework on how the methods relate to each other. Hopefully, this is a starting point to develop new architectures with benefits from the two “worlds”.

As we aim to bring together both research communities we begin this paper with an overview of the theoretical backgrounds of NNs and PBs. In chapter four we show a different interpretation of fully-connected layers by reformulating the underlying operations. Chapter five takes a similar approach but applies it to convolutional layers. Chapter six will introduce a prototype-based classification layer and a prototype inspired version of the convolution operation, often applied in NNs. Both methods rely on the different interpretations explored in chapter four and five. We discuss their benefits in chapter seven together with empirically gained insights where possible. Tips and tricks, discovered during our ongoing experiments are described in chapter eight. Chapter nine presents related approaches and chapter ten concludes and gives an overview of planned future work.

2 Introduction to prototype-based methods

Vector quantization is one of the most successful approaches for data clustering and representation as well as compression [12, 13]. One of the pioneers in vector quantization, R. M. GRAY stated [14]: “A vector quantizer is a system for mapping a sequence of continuous or discrete vectors into a digital sequence suitable for communication over or storage in a digital channel. The goal of such a system is data compression: to reduce the bit rate so as to minimize communication channel capacity or digital storage memory requirements while maintaining the necessary fidelity of the data.”

Most of the methods use the concept of prototypes and are therefore called PBs [15]. These methods are based on a set $W = \{\mathbf{w}_1, \mathbf{w}_2, \dots, \mathbf{w}_{N_w}\}$ of prototypes \mathbf{w}_k , usually in the \mathbb{R}^n , and a suitable dissimilarity or distance measure d [11]. The *prototype response vector* is defined as

$$\mathbf{d}(\mathbf{x}) = (d(\mathbf{x}, \mathbf{w}_1), \dots, d(\mathbf{x}, \mathbf{w}_{N_w}))^T \quad (1)$$

with the respective dissimilarity measure. Frequently, this is defined as the squared Euclidean metric

$$d_E^2(\mathbf{x}, \mathbf{w}) = (\mathbf{x} - \mathbf{w})^T (\mathbf{x} - \mathbf{w}). \quad (2)$$

The vector quantization mapping $\mathbf{x} \mapsto \kappa(\mathbf{x})$ takes place as a winner-takes-all (WTA) rule according to

$$\kappa(\mathbf{x}) = \arg \min \{d(\mathbf{x}, \mathbf{w}_k) | k = 1, 2, \dots, N_w\}. \quad (3)$$

realizing the nearest prototype principle with respect to the given dissimilarity. The value $\kappa(\mathbf{x})$ is called the index of the best matching (winner) prototype. According to the assignments $\kappa(\mathbf{x})$, a tessellation of the data space is induced by the Voronoï cells

$$V_k = \{\mathbf{x} \in \mathbb{R}^n | k = \kappa(\mathbf{x})\} \quad (4)$$

assigned to each prototype \mathbf{w}_k . It is frequently denoted as the receptive field of neural vector quantizers [16].

²We acknowledge that there are differences between mathematical distances and dissimilarities but will use the words interchangeably for simplicity in this contribution. For a detailed consideration we refer to [10, 11].

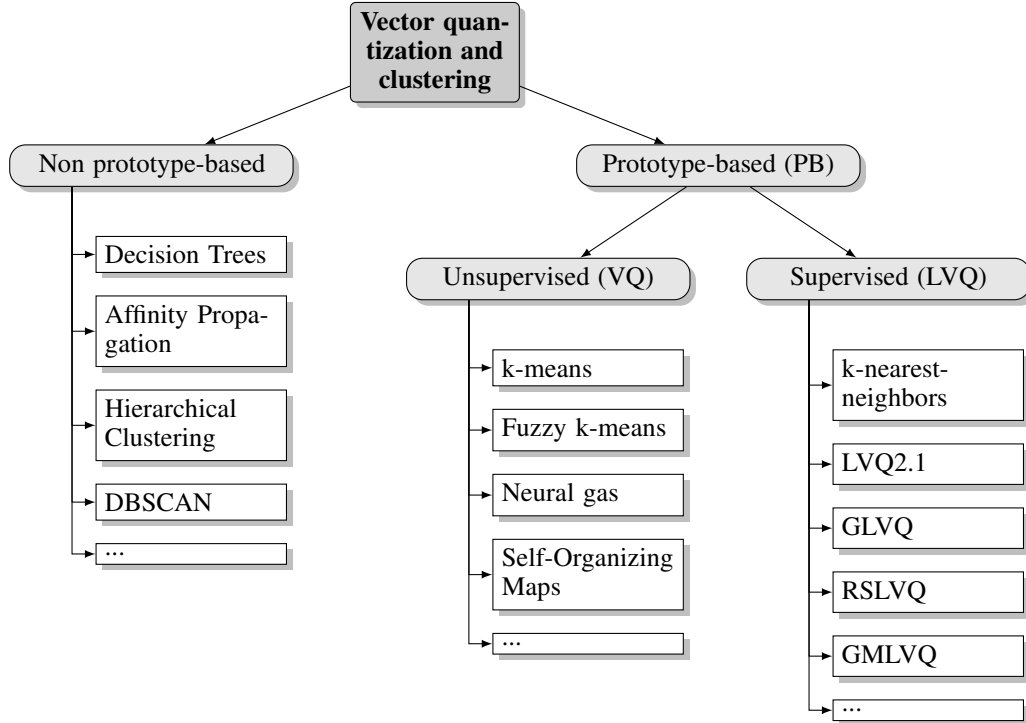


Figure 1: An overview of the general vector quantization/clustering methods landscape, explaining how different approaches relate to each other. It is important to note here that the unsupervised prototype-based vector quantization classifier referred to in this contribution is in fact only a part of the encompassing vector quantization methodology. For simplicity we have decided to use the name vector quantization and its abbreviation VQ to refer to the unsupervised prototype-based variant, as is done in most related work.

For unsupervised prototype-based vector quantization (VQ), each prototype is assumed to serve as a cluster center and hence, $\kappa(\mathbf{x})$ of the WTA-rule (3) delivers the cluster index. A model is trained either by a heuristically motivated update of the prototypes or by the optimization of a cost function [17, 18, 19]. After the training, the prototypes should be distributed in the data space such that the training dataset $\mathcal{X} \subseteq \mathbb{R}^n$ is well covered. Probably the most prominent example of VQ algorithms is k-means [19, 20]. In the past, several extensions and improvements of VQ methods were invented. For example methods with improved convergence behavior [21, 22], including neural gas [23], fuzzy variants where the crisp WTA-rule is replaced by a smoothed decision function [24, 25, 26, 27] and variants that use a different metric than the Euclidean distance [28, 29]. A systematic overview is given in [30].

The supervised counterpart to VQ is called Learning Vector Quantization (LVQ). It was initially developed for classification learning by T. KOHONEN in 1988 [31] and later extended [21]. In LVQ, each prototype \mathbf{w}_k is additionally equipped with a class label $c_k \in C = \{1, 2, \dots, N_C\}$ and the prototypes are distributed regarding a training dataset $\mathcal{X} = \{(\mathbf{x}, c(\mathbf{x})) \mid \mathbf{x} \in \mathbb{R}^n, c(\mathbf{x}) \in C\}$. The class of a given data point \mathbf{x} is defined as

$$\mathbf{x} \mapsto c(\mathbf{x}) = c_{\kappa(\mathbf{x})}, \quad (5)$$

yielding a crisp classification. Originally, the learning process of the prototypes was heuristically motivated, later it was refined to optimize a cost function which approximates the overall classification accuracy [32, 33]. Probabilistic variants of LVQ are the Robust Soft LVQ (RSLVQ [34]), the soft nearest prototype classifier [35] or the probabilistic LVQ [36] to name just a few. See Fig. 1 for an incomplete overview of the vector quantization landscape and its most prominent variants.

Non-standard metrics are also attractive for PBs [28, 37, 38, 39] since their incorporation provides a powerful modification. Generalized Matrix LVQ (GMLVQ [40]) supposes an adjustable dissimilarity measure, which is adapted during the training process. This adaption takes place in parallel to

the prototype learning. The dissimilarity measure is defined as

$$d_{\Omega}^2(\mathbf{x}, \mathbf{w}) = (\mathbf{x} - \mathbf{w})^T \Omega^T \Omega (\mathbf{x} - \mathbf{w}) \quad (6)$$

where the matrix $\Omega \in \mathbb{R}^{m \times n}$ is learned during the training. We denote this as Omega dissimilarity. The commonality of all these modifications is that the learning results in a suitable distribution of the prototypes in the data space.

The distance based perspective in prototype-based methods offers a clear understanding of the prototype principle and the WTA-rule provides many interpretation techniques e. g. biological excitation in neural maps or local area winner in Heskes-Self-Organizing-Maps [41, 42, 43]. It should be emphasized that the optimum assignment of a data sample \mathbf{x} to a prototype \mathbf{w}_k is achieved for $d(\mathbf{x}, \mathbf{w}_k) = 0$, which can be interpreted as a *lower bound*. This geometrical perspective makes the method attractive for outlier detection and related reject strategies [44, 45, 46, 47, 48, 49, 50].

3 Introduction to neural networks

In recent years, NNs and more specifically Convolutional Neural Networks (CNNs), gained a lot of attention due to their successes in a variety of difficult classification and regression tasks [5, 7, 6].

A neural multilayer feedforward network classifier can be decomposed into a feature extraction network concatenated with a classification network. The feature extraction network extracts a feature representation $f(\mathbf{x})$ from the input \mathbf{x} . This feature representation is consecutively passed into the network to obtain the final classification decision. For image classification, the extraction is usually realized using a stack of convolutional layers. The output $f(\mathbf{x})$ of the extraction network can then be seen as a feature stack (images of features). A reshaped representation of the feature stack is then the input layer of the classification network. Usually, this is defined as a multilayer perceptron network (fully-connected feedforward network). The ability to train the feature extractor and classifier at the same time is one of the main strengths of NNs and was instrumental to the adaption of this machine learning method.

In recent years a lot of techniques were developed to improve the accuracy and ease of training. Examples of these are: dropout [51], batch normalization [1], improved architecture [4, 5, 6] and different activation functions [2, 3]. In addition to this, newly available hardware support by GPU computing enabled the use of larger and deeper networks. For a more complete introduction and an overview of the history of NNs we refer to [52].

4 A different view on fully-connected layers

In the following, the relation between fully-connected layers (FCLs) and LVQ networks is explored. This allows to rewrite both of them using equivalent operations. This strategy is already described for different levels of abstraction in [53, 54, 55, 56, 57].

4.1 Relation between Euclidean distance-based PBs and FCLs

In the simple form, the output $\mathbf{o}(\mathbf{x})$, regarding a given input \mathbf{x} of a FCL of a feedforward network with trivial activation $id(\mathbf{x}) = \mathbf{x}$, can be written as

$$\mathbf{o}(\mathbf{x}) = \mathbf{A}\mathbf{x} + \mathbf{b} \quad (7)$$

where \mathbf{A} is the weight matrix and \mathbf{b} is the bias vector. Hence, the components are calculated according to

$$o_k(\mathbf{x}) = \langle \mathbf{a}_k, \mathbf{x} \rangle_E + b_k \quad (8)$$

where $\langle \mathbf{a}_k, \mathbf{x} \rangle_E$ is the Euclidean inner product and \mathbf{a}_k denotes the k -th row vector of the matrix \mathbf{A} .

Suppose that there is exactly one prototype \mathbf{w}_k that is responsible for each class and that the class c_k of this prototype is k , i. e. $c_k = k$ with $k \in \{1, \dots, N_C\}$ and $N_W = N_C$.³ Based on these assumptions, the prototype response vector in (1) can be written as

$$\mathbf{d}(\mathbf{x}) = (d_E^2(\mathbf{x}, \mathbf{w}_1), d_E^2(\mathbf{x}, \mathbf{w}_2), \dots, d_E^2(\mathbf{x}, \mathbf{w}_{N_C}))^T \quad (9)$$

³The restriction to one prototype per class can be easily relaxed and a similar formulation can be obtained.

for the squared Euclidean distance measure.

However, this formulation (9) of the prototype response shows a *computational disadvantage*: for parallel computation of the response vector $\mathbf{d}(\mathbf{x})$, multiple copies of the input \mathbf{x} are needed, in order that each component $d_k(\mathbf{x}) = d_E^2(\mathbf{x}, \mathbf{w}_k)$ can be calculated independently. Hence, the respective storage requirements grow with the number of classes/prototypes. This bottleneck of the naive approach limits the scalability of LVQ to large networks or to networks with a huge number of classes.

By considering the identity

$$d_E^2(\mathbf{x}, \mathbf{w}_k) = \langle \mathbf{x}, \mathbf{x} \rangle_E - 2 \langle \mathbf{x}, \mathbf{w}_k \rangle_E + \langle \mathbf{w}_k, \mathbf{w}_k \rangle_E \quad (10)$$

for the Euclidean distance, these limitations can be overcome. For this purpose, all prototypes are collected into a matrix $\mathbf{W} \in \mathbb{R}^{N_C \times n}$ in order that

$$\mathbf{W} = (\mathbf{w}_1 | \mathbf{w}_2 | \dots | \mathbf{w}_{N_C})^T$$

is valid. Now Eq. (9) is equivalent to

$$\mathbf{d}(\mathbf{x}) = -2\mathbf{W}\mathbf{x} + \mathbf{b}(\mathbf{x}, \mathbf{W}) \quad (11)$$

with

$$\mathbf{b}(\mathbf{x}, \mathbf{W}) = \left(\|\mathbf{x}\|_2^2 + \|\mathbf{w}_1\|_2^2, \|\mathbf{x}\|_2^2 + \|\mathbf{w}_2\|_2^2, \dots, \|\mathbf{x}\|_2^2 + \|\mathbf{w}_{N_C}\|_2^2 \right)^T \quad (12)$$

and thus the parallel calculation of $\mathbf{b}(\mathbf{x}, \mathbf{W})$ requires only copies of the single value $\|\mathbf{x}\|_2^2$ instead of the full vectors \mathbf{x} .

It can be observed that the computation of the response vector $\mathbf{d}(\mathbf{x})$ according to (11) is structurally equivalent to the output (7) of a FCL with trivial activation $id(\mathbf{x}) = \mathbf{x}$: Both methods apply a linear transformation to the input vector and add a bias term. The difference is that in a FCL (7) the bias term \mathbf{b} is a trainable parameter, whereas in LVQ the bias term $\mathbf{b}(\mathbf{x}, \mathbf{W})$ depends dynamically on the prototypes and the current input vector.

4.2 Relation between the Omega dissimilarity and two FCLs

A multilayer perceptron that combines multiple FCLs can be seen as a repeated application of Eq. (7), using a generally nonlinear activation function ϕ (e. g. the Rectified Linear Unit - ReLU [2] or sigmoid).

Consider a network with two FCLs and trivial activation in the second layer. The output can be defined as

$$\mathbf{o}(\mathbf{x}) = \mathbf{A}\phi(\mathbf{A}_1\mathbf{x} + \mathbf{b}_1) + \mathbf{b} \quad (13)$$

where \mathbf{A}_1 and \mathbf{b}_1 are the parameters of the first layer. This shows that the first layer applies an affine transformation of the input vector \mathbf{x} , followed by a transformation according to the activation $\phi(\mathbf{x}) = (\phi(x_1), \dots, \phi(x_n))^T$. Afterwards, the vector $\phi(\mathbf{x})$ serves as the input to the second layer, which delivers the output by following the rule (7). Hence, the first layer can be interpreted as nonlinear input transformation of \mathbf{x} due to the nonlinear activation function.

For comparison, consider a variation of the Omega dissimilarity d_Ω of GMLVQ from (6), i. e. the measure

$$\delta_\Omega^2(\mathbf{x}, \mathbf{w}) = (\Omega\mathbf{x} - \mathbf{w})^T (\Omega\mathbf{x} - \mathbf{w}) \quad (14)$$

is investigated. The data vector \mathbf{x} is first linearly projected by the projection matrix Ω into the projection space and consequently the prototypes are defined within this space. The initial projection $\Omega\mathbf{x}$ can be interpreted as a FCL without bias and with trivial activation. With the application of Eq. (11) still being valid, the application of δ_Ω can be understood as a two FCL network with the constraints described above. Furthermore, this perspective can be generalized to the measure

$$\mu_\Omega^2(\mathbf{x}, \mathbf{w}) = (\phi(\Omega\mathbf{x} - \mathbf{b}) - \mathbf{w})^T (\phi(\Omega\mathbf{x} - \mathbf{b}) - \mathbf{w}) \quad (15)$$

as suggested in [58]. In this way a complete correspondence is obtained between the Omega dissimilarity and a multilayer perceptron using two FCLs.

5 A different view on convolutional layers

In the following, we show how a matrix multiplication can be expressed in terms of convolution operations. In CNNs the convolutional layer is not defined as a mathematical convolution, instead it is a mathematical cross-correlation also denoted as sliding dot product (inner product) [59]. Nevertheless, we will refer to it as convolution for simplicity.

In this chapter we suppose that $\mathbf{x} \in \mathbb{R}^{w \times h \times c}$ is a feature stack of size $w \times h \times c$ and $\mathbf{k} \in \mathbb{R}^{w_f \times h_f \times c}$ a convolutional kernel. Suppose that $\mathbf{x}_{ij} \in \mathbb{R}^{w_f \times h_f \times c}$ is the window at the pixel position i, j of \mathbf{x} where the response with the kernel \mathbf{k} should be evaluated. Then, the output of the convolution $\mathbf{x} * \mathbf{k}$ at pixel position i, j is given by

$$\mathbf{x} * \mathbf{k}|_{ij} = \tilde{\mathbf{x}}_{ij}^T \tilde{\mathbf{k}} \quad (16)$$

where $\tilde{\mathbf{x}}_{ij}$ and $\tilde{\mathbf{k}}$ are replicas of \mathbf{x}_{ij} and \mathbf{k} in vector shape, i. e. $\tilde{\mathbf{x}}_{ij} \in \mathbb{R}^{w_f \cdot h_f \cdot c}$ and $\tilde{\mathbf{k}} \in \mathbb{R}^{w_f \cdot h_f \cdot c}$.

Like usual in CNNs, we filter the images with a stack of filters. Assume there are N_f filters of shape \mathbf{k} collected in a tensor of the shape $w_f \times h_f \times c \times N_f$. Then, the convolution with all these filters can be seen as a matrix multiplication. More precisely, it is a linear transformation of the vector collected over a sliding window from $\mathbb{R}^{w_f \cdot h_f \cdot c} \rightarrow \mathbb{R}^{N_f}$ by

$$\tilde{\mathbf{K}} \tilde{\mathbf{x}}_{ij} \quad (17)$$

where $\tilde{\mathbf{K}} = \left(\tilde{\mathbf{k}}_1 | \tilde{\mathbf{k}}_2 | \dots | \tilde{\mathbf{k}}_{N_f} \right)^T$ is the matrix of the vectorized filters $\tilde{\mathbf{k}}_l$.

If the convolution operation is equipped with the additional bias term $\tilde{\mathbf{b}}_l$ for each kernel, then this is equivalent to a linear transformation of the form (17) followed by a vector shift, i. e. the resulting operation

$$\tilde{\mathbf{K}} \tilde{\mathbf{x}}_{ij} + \tilde{\mathbf{b}}$$

is an affine transformation.

To summarize, the general convolution operation of CNNs is an affine transformation of each sliding window with the same transformation (known as shared weights).

6 Prototype-based neural network layers

In the previous sections we have shown how NNs and the prototype-based learning methods LVQ and VQ relate to each other. Using these relations, we propose two prototype-based layers to be used in NNs in the following section.

6.1 LVQ layers as final classification layers

As mentioned in Sec. 4, the implementation of LVQ as final classification network of a NN, split into feature extraction and classification, is straightforward. During the training of the NN the prototypes are trained in parallel with the feature extraction layers, using the output of the feature extraction layer as input to the prototype-based model. At inference, the distance between the output of the feature extraction layer and all learned prototypes is used for classification. This requires the selection of a differentiable loss function and distance measure.

Below, two special cases of LVQ classification layers are proposed and their loss functions are defined.

RSLVQ In general, the output vector $\mathbf{o}(\mathbf{x})$ of (7) in the last FCL of a NN is element-wise normalized by the softmax activation (also denoted as Gibbs measure/distribution) given

$$\hat{\mathbf{p}}(\mathbf{x}) = \text{softmax}(\mathbf{o}(\mathbf{x}))$$

with $\hat{\mathbf{p}}(\mathbf{x}) \in [0, 1]^{N_c}$ being a probability vector of the estimated class probabilities and the softmax function defined as

$$\text{softmax}(z_k) = \frac{\exp(z_k)}{\sum_i \exp(z_i)} \quad (18)$$

for vectors $\mathbf{z} = (z_1, \dots, z_n)^T$. The training of the network is usually realized applying the cross entropy loss for the network class probability $\hat{\mathbf{p}}(\mathbf{x})$ and the true class probability $\mathbf{p}(\mathbf{x})$.

Robust Soft Learning Vector Quantization (RSLVQ) was introduced by SEO and OBERMAYER [34] as a probabilistic version of LVQ. RSLVQ defines the prototypes as centers of Gaussian densities and the whole machine learning model as Gaussian density mixture model. During the learning, the prototypes are adjusted to approximate the class probability densities of the data. This is achieved via a maximum log-likelihood optimization of the class dependent Gaussian mixture model. For that, the prototype response vector $\mathbf{d}(\mathbf{x})$ of distance values from (11) is transformed into a probability vector via

$$\hat{\mathbf{p}}(\mathbf{x}) = \text{softmax}(-\mathbf{d}(\mathbf{x})) \quad (19)$$

in the RSLVQ network, which obeys a Gaussian probability in presence of the squared Euclidean distance. It turns out that the maximum log-likelihood loss function of RSLVQ is equivalent to the cross entropy loss between $\hat{\mathbf{p}}(\mathbf{x})$ and $\mathbf{p}(\mathbf{x})$ [36].

Hence, a RSLVQ classifier can be interpreted as fully-connected softmax classification layer with the particular bias $\mathbf{b}(\mathbf{x}, \mathbf{W})$ according to (12). It is worth noticing, that the projection distance $\delta_\Omega^2(\mathbf{x}, \mathbf{w})$ from (14) or its nonlinear counter part $\mu_\Omega^2(\mathbf{x}, \mathbf{w})$ from (15) can also be used in RSLVQ. Furthermore, the WTA-rule in RSLVQ results into a maximum probability decision regarding the probability vector $\hat{\mathbf{p}}(\mathbf{x})$ as it is applied for FCLs.

GLVQ As mentioned previously, a prominent LVQ network is the generalized LVQ architecture (GLVQ) with a loss function approximating the overall classification error [32], which realizes a hypothesis-margin maximizer [60]. Given a prototype response vector $\mathbf{d}(\mathbf{x})$ regarding an input \mathbf{x} , the loss is evaluated as

$$\frac{d_{c(\mathbf{x})}(\mathbf{x}) - d_{\bar{c}(\mathbf{x})}(\mathbf{x})}{d_{c(\mathbf{x})}(\mathbf{x}) + d_{\bar{c}(\mathbf{x})}(\mathbf{x})} \quad (20)$$

where $\bar{c}(\mathbf{x})$ is the class of the closest prototype of an incorrect class regarding \mathbf{x} . This loss is not comparable with the commonly used NN losses. However, as already discussed in Sec. 4.2, applying the projection distance $\delta_\Omega^2(\mathbf{x}, \mathbf{w})$ from (14) or its nonlinear counter part $\mu_\Omega^2(\mathbf{x}, \mathbf{w})$ from (15) in LVQ results in a network model with two FCLs which can be trained by using (20).

6.2 VQ layers as prototype convolution operation

Similar to Sec. 5, we now suppose a convolutional kernel $\mathbf{k} \in \mathbb{R}^{w_f \times h_f \times c}$. However, rather than considering the kernel \mathbf{k} as a learnable filter, we consider the kernel as a learnable (kernel-)prototype. Then, the filter response of the convolution operation is the distance between the sliding window and the kernel-prototype. We denote the convolution operation in combination with a kernel-prototype using the \otimes sign and refer to it as *kernel-prototype convolution*.

Using the Euclidean distance, expressed in terms of dot products (10), the kernel-prototype convolution $\mathbf{x} \otimes \mathbf{k}$ at image position i, j yields

$$\mathbf{x} \otimes \mathbf{k}|_{ij} = \|\tilde{\mathbf{x}}_{ij}\|_2^2 - 2\tilde{\mathbf{x}}_{ij}^T \tilde{\mathbf{k}} + \|\tilde{\mathbf{k}}\|_2^2$$

and for the whole image

$$\mathbf{x} \otimes \mathbf{k} = \mathbf{x}^2 * \mathbf{1} - 2\mathbf{x} * \mathbf{k} \oplus \|\mathbf{k}\|_2^2 \quad (21)$$

where $(\cdot)^2$ is the component-wise square, $\mathbf{1}$ is a kernel of ones with the shape equal to \mathbf{k} and \oplus is the component-wise addition. This equation can be efficiently evaluated and hence, a kernel-prototype of arbitrary kernel-size can be convoluted over an input. In the previous example, the kernel-prototype is equivalent to a $w_f \cdot h_f \cdot c$ dimensional vector. Thus, the kernel-prototype convolution measures the distance to the kernel-prototype in a $w_f \cdot h_f \cdot c$ dimensional space.

For a kernel-prototype convolution the number of filters N_f equals the number of kernel-prototypes N_W . Each feature map in a kernel-prototype convolution therefore corresponds to the distance of the input to a different kernel-prototype. To better reflect the output of the kernel-prototype convolution, we refer to each feature map as *dissimilarity map* and the resulting whole feature stack as *dissimilarity stack*. The encoding of a given input into a dissimilarity representation is equivalent to a counter-propagation network representation [61, 62].

To strengthen the relation between the normal convolution and the kernel-prototype convolution a bias term can be added. For this purpose, we consider the equation of a n -ball

$$B_r(\mathbf{w}) = \{\mathbf{x} \in \mathbb{R}^n | d(\mathbf{x}, \mathbf{w}) < r\}$$

with radius r around the (usual) prototype \mathbf{w} . Thus, the expression

$$r^2 - \mathbf{x} \circledast \mathbf{k} \begin{cases} > 0 & \text{if the vector of the sliding window is inside } B_r(\tilde{\mathbf{k}}) \\ \leq 0 & \text{else} \end{cases}$$

returns a positive value if a sliding window is inside the spanned n -ball of a (usual) prototype and a negative value otherwise. The evaluation of multiple filters N_f can therefore be seen as determining for each point in which n -ball it is located. By only assigning a positive score when a point is within a n -ball, the kernel-prototype convolution can be interpreted as a quantization. These properties will be further explored in the following sections.

It is important to note, that it is still possible to work directly on the dissimilarity stack. Moreover, the application of a convolutional filter, with a linear activation before a kernel-prototype convolution without a bias, is similar to measuring with an Omega dissimilarity, as discussed in section 4.2 regarding two FCLs.

7 Potential benefits

PBs and NNs have different benefits over each other in classification tasks. In this section we will provide an overview of how we think these benefits will transfer when PBs and NNs are combined. As this is still an active area of research we do not intent this to be a complete overview. Where possible, we will provide examples of how these benefits can be experienced in an experimental setting.

7.1 Feature extraction pipeline for LVQ

In terms of accuracy, it is not necessary to discuss about which machine learning method has a broader application. NNs are impressively powerful in solving real world image tasks like object detection or object classification. Due to the high complexity of such tasks, plain LVQ cannot provide a satisfactory accuracy. The power of NNs results from their usually underlying deep architectures and the training of the feature extraction and the classification layers in an end-to-end fashion. The joint training of these two parts is usually not considered in PBs.

However, using the methods described above we were able to train a NN with prototype-based layers in an end-to-end fashion on both MNIST and Tiny ImageNet. For MNIST a relatively small network was trained to a validation accuracy of 99%. For Tiny ImageNet⁴ an altered version of the classic ResNet with 50 layers was adapted to use a RSLVQ classification layer. We were able to train the 200-class dataset achieving a validation accuracy of 67.4%. At the same time we were able to reduce the number of parameters by 25% by replacing the FCLs in the ResNet by the RSLVQ architecture. This is, to the best of our knowledge, the first time that a prototype-based classifier was trained in end-to-end fashion on a dataset with such a large number of classes.

7.2 Distance-based interpretations in NNs

Even though the research community around LVQ and VQ is relatively small compared to the NN society, it is a very active area of research and the researchers have produced useful techniques and interpretations around the methods. By injecting PBs into NNs it is possible to transfer the interpretation techniques from PBs in NNs. There are several discussions about the benefits of interpretable NNs. One might be simply the fact of human nature: our aim to understand the things surrounding us. From the perspective of function applications in safety critical system like autonomous driving, we want to certify functions and want to define validation and verification standards. Of course, this requires some understanding and interpretability of the model in use. Otherwise it is hard to define the positive operational range of the function.

⁴Tiny ImageNet is a downsampled subset of the ImageNet dataset, see <https://tiny-imagenet.herokuapp.com/>

Definition of the distance and dissimilarity measure The simplest and most powerful property of PBs is their clear geometrical motivation and interpretation. A distance is a well defined expression, capturing a clear definition about what is close and allowing for a direct ordering of points in terms of closeness. Mathematically speaking, the lower bound of distances is well-defined, it is simply zero. In traditional NNs there is not such a strong interpretation of the layer outputs. Moreover, the inner product is unbounded, which may lead to an unbounded output for special choices of activation functions like linear or ReLU. Using the proposed kernel-prototype convolutional layers instead of traditional layers can bring this strong definition and bound into the NNs.

For example in NNs it is hard to get an understanding of what the filter response of a convolutional layer is or what it represents. Using a kernel-prototype convolution enables to find a stronger interpretation: The filter response of a kernel-prototype convolution conveys the distance between the considered convolution window and the prototype. In addition to this interpretation ability for the response, the suggested approach allows to compare filter responses with each other. This makes it possible to detect which features are most appropriate for a certain pixel position.

Class-typical prototypes In traditional prototype-based learning methods the prototypes are supposed to capture the “ideal” representation of the data points of a certain class. A prototype can be seen as an abstraction of the class that it is demanded to represent. It yields a good approximation of the data contained in the belonging receptive field. Hence, a prototype can be interpreted in the same way as the original data. An example for this is speech recognition: if an LVQ model was trained to recognize certain words, the resulting prototypes are easy to understand because they represent speech. This is particularly the case if median variants of PBs, which restrict the prototypes to be data points, are used [63].

However, in an end-to-end approach with trainable feature extraction and a final LVQ layer, this property can be lost. This is not solely an issue of LVQ in combination with end-to-end feature extractors as it can also occur in plain LVQ. It is called the trade-off between generative and discriminative prototypes [64]. Generative prototypes are prototypical for the data and lie inside the point cloud of their class. Discriminative prototypes can lie outside the class’s point cloud but maintain a better decision border than when they lie inside.

Adding a regularization term to the used cost function can force the prototype classifier to be class-typical and we can alleviate this issue [65]. Furthermore, if the data mapping components like (15) or any deep preprocessing network are included in the LVQ method, the regularization term can be used to map the data in such a way that data points within a receptive field follow a Gaussian distribution in the projection (feature) space. In that case, the Kullback-Leibler divergence between the projected local data distribution inside a receptive field of a prototype and a Gaussian in the projection space should be minimized.

First experimental numerical results show that using this latter regularization approach forces the prototypes to be both generative and discriminative in the projection space at the same time.

Feature importance GMLVQ is known for a strong interpretability property of the Ω -matrix. The product matrix $\Lambda = \Omega^T \Omega$ in (6) is denoted as classification correlation matrix [33]. A trace-normalization preserves Λ to be a matrix where the resulting entries are understood as correlation values of the feature space dimensions. The correlation information is used to apply precise feature selection and to perform a pruning after the training. This normalization acts as a constraint during the training. Using the outlined relation of the dissimilarity $\delta_{\Omega}^2(\mathbf{x}, \mathbf{w})$ from (14) in FCLs, more interpretability can easily be gained in the weight matrices of these FCLs, particularly if a deep structure is considered to feed the FCLs.

Interpretation techniques for NNs Recent results have turned NNs from a black-box into a gray-box, relaxing the accusation that NNs are not interpretable [66]. A wide range of powerful tools to analyze convolutional layers and highlight important regions in an image have become available. With small modifications the same techniques can also be available for PBs. This has already been shown in [67], where decoder networks were successfully applied to decode a vectorial output (e. g. the prototypes) into a representation in the input space.

7.3 Prototype-based robustness in NNs

The search for networks that are robust against adversarial attacks has grown a lot in recent years. Nevertheless, almost each defense can still be broken with a suitable attack [68]. This observation seems to be plausible under the scope of the No-Free-Lunch theorem [69]. As mentioned earlier however, PBs are known for being robust. By using prototype-based layers in multilayer networks we therefore expect the network to become more robust against adversarial examples.

This expectation is mathematically supported by strong theoretical results regarding the convergence of prototype-based methods [70, 71], hypothesis margin optimization by LVQ networks [60] and other aspects like information theoretic properties, Bayesian decision theory for LVQ networks and more [72, 73, 74, 48]. These results do not improve the robustness of the LVQ methods automatically, but the theoretical results provide mathematical certainty.

Below we will discuss one property of PBs and one commonly used approach that we think can contribute to the robustness.

Homogeneity As outlined previously, LVQ networks provide a Voronoï tessellation of the input/feature space according to Eq. (4) in dependence on the prototype distribution. Inside each Voronoï cell V_k the class decision is homogeneous according to the class assignment rule (5). The local n -balls $U_{\varepsilon(k)}(\mathbf{w}_k)$ around a prototype as approximations of Voronoï cell V_k are defined in such a way that

$$\varepsilon(k) = \operatorname{argsupre\,mum}_{\varepsilon} \{ U_{\varepsilon(k)}(\mathbf{w}_k) \subset V_k \}$$

is valid, meaning that the maximum n -ball is fully contained in the Voronoï cell V_k . Then the n -balls are disjunctive, i.e. $U_{\varepsilon(k)}(\mathbf{w}_k) \cap U_{\varepsilon(j)}(\mathbf{w}_j) = \emptyset, \forall k \neq j$ and the classification decision inside each ball is homogeneous.

We believe and argue that the verification and validation of safety critical functions based on classifier decisions will be much more clear (and therefore much more accepted), if a mathematically precise description of regions with homogeneous classification decisions is possible. This argumentation is underpinned by several recently published proofs for robustness of NNs, where approximations of the n -balls are used with the underlying assumption regarding the valid classification decision homogeneity [8, 75].

WTA and hard assignments The WTA-rule commonly used in PBs combined with the crisp classification assignments offers a level of mathematical abstraction that is not found comparably in NNs. We believe that without a certain level of abstraction allowed by homogeneous regions, small perturbations in the input will result in a large difference in the output.

For this reason we experimented with hard assignment activations regarding the kernel-prototype convolutions in our recent simulations: the respective outputs are binary maps of zeros and ones, so far resulting in promising results. Additionally, the prototype-based classification layer also adds a certain level of abstraction. The ResNet with 50 layers discussed in Sec. 7.1 was ranked top 20 of overall 312 participants in the NeurIPS’2018 adversarial vision challenge, in which robust models were validated using novel adversarial attacks.

7.4 Reject options in NNs

A further issue regarding robustness in NNs is the rejection of unclassifiable data, such as adversarial examples that can no longer be recognized. While a lot of work has been done on outlier detection in NNs [47, 76, 77, 45, 49, 78, 79], rejecting those outliers is not common in the defense against adversarial examples. On the other side outlier rejection is a very common topic in prototype-based learning [44, 80]. Most of these reject strategies are based on the the fundamental property of dissimilarity measures to always be greater or equal zero and that $\mathbf{x} = \mathbf{y}$ implies $d(\mathbf{x}, \mathbf{y}) = 0$.⁵ In addition to this there are also some reject strategies used in prototype-based learning based on Bayesian theory and proven to be Bayes optimal [46, 48].

We have so far experimented with applying two reject strategies from LVQ in NNs using prototype-based layers. The first one spans n -balls around the prototypes and considers points outside the balls

⁵Other properties of distance measures can be relaxed for general dissimilarity measures [11].

as outliers, see [44] for a possible termination of the radii. The second one uses a misclassification loss to train the network over minimizing the classification error rate and the reject rate [81]. The idea is to introduce misclassification costs λ_e , reject-costs λ_r and a reject strategy in the network. Via tuning of the network parameters, the network learns to optimize a trade-off between misclassifying and rejecting inputs.

7.5 Shared losses and regularizations between PBs and NNs

The NN community is open to new developments, even without a precise mathematical foundation being presented if a benefit in performance can really be expected. Entrusting empirical justifications, the community allows quick iterations and improvements to be made, which is, in our view, an important factor in the recent success of NNs. It allowed researchers to think about specialized loss functions, regularization terms or particular optimizers for the considered problem, which can be easily adapted to new problems.

In contrast, most LVQ variants are optimized according to the underlying GLVQ-loss, which is a smooth approximation of the classification accuracy but, as already mentioned above, corresponds to a hypothesis margin maximizer. Probabilistic variants like RSLVQ rely on log-likelihood ratios, which turn out to be equivalent to the cross entropy loss under mild assumptions [36]. We wish that the PB community is inspired by the rapidly developing NN-world to think towards adaptation for vector quantization models. A respective example is the incorporation of dropout techniques for GMLVQ for stability analysis [82].

Nonlinearities Nonlinearities in the form of activation functions play a key role in both PBs and NNs. Both methods however rely primarily on different activation functions. For NNs the ReLU function is mostly used for intermediate layers and the softmax function for the final classification layer. For PBs, the focus has been primarily on the sigmoid and linear activation function. However, recently the swish function has been showed to slightly improve the classification of many standard datasets over the ReLU function in NNs [83]. This shows the benefit that can be gained from switching to a different activation function and is a motivation to incorporate activation functions such as ReLU in PBs and vice versa. Additionally, the use of ReLU for GLVQ classification layers in NN has already been shown [57].

Instead of using the NN inspired activation functions for the final classification only, they can also be applied to the kernel-prototype convolutional layer. An example of this is the usage of a ReLU function to clip the convolutional layer with bias. By doing so, positive values are assigned to points inside the n -ball $B_r(\mathbf{w}_k)$ of a prototype and zeros to points outside. The largest value is then defined by the bias, with larger values when the vector is closer to the prototype. Furthermore, we experiment with applying the softmax activation function over the channels of the dissimilarity stack to assign cluster probabilities to each pixel position. Equivalently, we use the sigmoid activation to get cluster possibilities instead of probabilities. This way, a value greater than 0.5 is assigned if a point is inside the n -ball of a prototype and lower otherwise.

Regularization Similar to nonlinearities, using prototype-based layers allows to share regularization techniques developed for NNs in PBs, like the l_1 -norm regularization term known from NNs to the bias term of kernel-prototype convolutions. The idea is to keep the trust region around a prototype as small as possible. During the training the network automatically turns prototypes off which are not used in the following layers. After the training the prototypes can be removed without any effect on the network performance. Similar approaches were presented in [84] for sparse feature utilization in GMLVQ.

The other way around, regularization techniques known in GMLVQ can provide new aspects for NNs. An example of this is to apply the eigenvalue regularization known for GMLVQ (see [85, 86]) for a two-layer network of FCLs, which can potentially reduce the over-simplification effect in the projection space.

7.6 Arbitrary input dimensions and structured data for NNs and vector quantization

In [87] a capsule concept was proposed to work on tensor signals between neurons/perceptrons. The output over all neurons of a FCL can be considered as a vector. In a capsule network, the

entities that are transmitted along a connection between two capsules are arbitrary tensors and thus, the collected output of a capsule layer is a tensor and therefore not longer restricted to be a vector. This concept allows to think about new processing steps inside and between capsules and hence to go beyond vectorial operations. This is however not a new concept in machine learning, but rather a well established property of PBs: a simple example is to use a matrix as the input to a VQ network, then the prototypes are matrices as well and hence, a respective matrix dissimilarity has to be chosen [88]. However, using more complex dissimilarity measures it is also possible to model prototypes as affine subspaces of the input space [89, 90].

8 Some tricks to successfully train prototype-based neural network layers

Merging both methods does not only bring their benefits but also their difficulties, e. g. that the PBs are hard to train compared to NNs. However, a variety of techniques have already been developed in both research areas that can also be used in the merged methods to alleviate (part) of these difficulties.

Prototype initialization The training of PBs depends usually on a good initialization [91, 92, 93]. For this reason, instead of random initialization, we use two different strategies which are frequently used to train VQ/LVQ networks:

- the prototypes are initialized as randomly chosen input vectors
- the prototypes are initialized as centers of a k-means algorithm or neural gas

A similar strategy works for a proper initialization of the biases in a prototype convolution.

Prototype regularization As noted in [23], one problem in learning prototypes is that they often remain unchanged because of an initialization in data regions of low density. To avoid this, neighborhood cooperativeness has been established using an external grid structure following the dynamics of learning in neural maps in cortical brain areas [21]. A similar concept without external grid is the neural gas quantizer proposed by MARTINETZ and SCHULTEN with a winning rank dependent neighborhood cooperativeness [23]. We use this method in our experiments by defining the gradient back-flow of VQ layers in the update step as rank dependent.

For some of the regularization and loss terms described in this report it is needed to estimate the data distribution over the training dataset. Since the network is optimized by stochastic gradient descent learning, the statistics over the whole dataset cannot be estimated during run-time. This can be compensated via moving averages/ moving variances. Additionally, we frequently prefer to perform a zero de-biasing according to [94] to avoid biased gradients.

Hard assignment derivative As discussed in Sec. 7.3, we carried out experiments using discrete outputs for the prototype-based layers. Unfortunately, a network with discrete output values is not differentiable. Thus, we needed to define approximated gradients. The hard assignments are defined and trained in the following way:

1. In case of a prototype convolution without bias, the output value of each pixel is defined as one for the closest prototype and zero for all the other prototypes. Thus, the dissimilarity stack becomes a stack of unit vectors. This hard probability assignment can be approximated by applying the function (19) with a kernel width σ equivalent to the sigmoid function. If σ tends to be zero, the softmax function approximates a hard probability assignment.
2. In case of a prototype convolution with bias, the Heaviside step function is applied as activation for each dissimilarity value. Thus, points inside the n -ball $B_r(\mathbf{w}_k)$ of a prototype are assigned to one and zero otherwise. Again, this hard possibility assignment can be approximated by applying the sigmoid function.

In the forward pass of the network, the hard output assignments are transmitted to the next layer. In the backward pass of the network, the gradient is approximated by the softmax and sigmoid function respectively. By adaption of the kernel width σ the quality of these approximations can be controlled. This strategy is similar to the gradient-straight-through approach applied in [55].

Theoretically, the approach 2. is capable to handle more complex tasks. The reason is that in this approach, the encoding for the following layer is not restricted to unit vectors. More precisely, in approach 1. N_W different encodings can be created in the probability stack whereas the number of distinguishable encodings in 2. is 2^{N_W} .

9 Related work

One of the first contributions reporting an approach for the fusion of LVQ with NNs is [53]. Later on, the idea was formulated more precisely [54]. In [57], a fused network was applied to train a network on MNIST and Cifar10. They showed a way how a regularization term can be used to get a generative and discriminative model at the same time. Moreover, they exemplarily applied a reject strategy and showed that the concept of incremental learning is also applicable.

The definition of a network directly on the discrete cluster representation of a VQ layer was first mentioned in the VQ-Variational-Autoencoder (VQ-VAE) [55]. There, the output of the VQ is a map where a pixel has the integer number k of the closest prototype. Moreover, the output is defined as the latent space of the VQ-VAE. The method was trained via the gradient-straight-through method. The obtained results are promising. Nevertheless, the authors were unable to train the model from scratch even with soft-to-hard assignment proposed in [56]. We made similar observations like in [55] for our simulations performed so far. If we train using soft-to-hard assignments, the model is able to invert the continuous relaxations. We also observed that training by a simple gradient-straight-through approximation is not stable, when the model is trained from scratch. However, our proposed gradient approximation is working well for many performed settings, either to train from scratch or on a pre-trained network.

In the VQ-VAE, the closest prototype at each pixel position is used directly as the input to the decoder. This architecture can easily be fitted into our framework: it is equivalent to applying a 1×1 kernel-prototype convolution without bias to the final layer of the encoder, followed by a hard class assignment (see Sec. 8, method 1). Afterwards a 1×1 transposed convolution has to be applied over the unit vector stack with the number of filters equaling the prototype dimension. If the prototypes are used as inputs for the decoder, the weights in the 1×1 convolution can be defined as the prototypes from the kernel-prototype convolution. Thus, the two convolutional layers share the weights. Instead of sharing the weights, we propose to just initialize the weights of both layers equivalently and then train the kernels independently. If the prototype representations are appropriate to start the decoding, we can assume that these weights will be discovered by the training anyways. In fact, this framework is more generic than the sharing weights approach, because it does not raise the question how the prototypes are pushed to the decoding network if the kernel-prototype convolution is defined via a kernel size greater than 1×1 to include neighborhood relations in the quantization process.

In the paper [67] a framework is presented to fuse VQ/LVQ with capsule networks [87]. We spend a lot effort to analyze this network architecture and corresponding routing mechanism. First of all, we found that this network is not able to transmit the message that an attribute is not present in the given representation to the next layer. For example, assume the problem of discrimination between cats and boats. Obviously, the presence of the attribute water is of interest for the class boats and its absence is important for the class cats. Since the routing is driven by preferring signals with a small distance, the signal from the water prototype indicating that water is not present (big distance) will be vanished in the routing process by assigning small routing probabilities to the next layer. Thus, the network decision is driven by present entities only. Moreover, we observed that the network learns to ignore the routing process by pushing the whole signal flow over just one prototype. The following layers were just working on this one hot signal (or a few of them) instead of using the whole network capacity.

10 Conclusion

In this conceptual paper we presented relations between VQ/LVQ and NN approaches for classification and how they fit into each other. We summarized important concepts from both theoretical fields, which are potentially not common/unknown in the other field. As major contribution we showed, how an Euclidean distance calculation can be expressed in terms of convolution operations

in the NN sense. This and the computation of the Euclidean distance in terms of a dot product are essential steps towards efficient computation schemes for prototype-based neural network layers. Using these approaches we were able to train a ResNet50 + LVQ network on Tiny ImageNet with 200 classes without any scalability problems.

Right now, we are evaluating architectures with our proposed layers and training pipelines. At several steps in the paper we mentioned current results without presenting precise quantities because the evaluation is still going on. The presentation of the experimental results will be part of our upcoming contribution.

Overall, we hope that this overview is stimulating for researchers from both communities to study together on fused models and to discover how established frameworks from one method can be incorporated into the other. We also hope that this contribution serves a good starting point for research and cites the recent trends from both sides.

References

- [1] Sergey Ioffe and Christian Szegedy. Batch Normalization: Accelerating Deep Network Training by Reducing Internal Covariate Shift. *CoRR*, abs/1502.0, 2015.
- [2] X. Glorot, A. Bordes, and Y. Bengio. Deep sparse rectifier neural networks. In G.J. Gordon and D.B. Dunson, editors, *Proceedings of the Fourteenth International Conference on Artificial Intelligence and Statistics (AISTATS-11)*, number 15, pages 315–323. Journal of Machine Learning Research - Workshop and Conference Proceedings, 2011.
- [3] P. Ramachandran, B. Zoph, and Q.V. Le. Swish: A self-gated activation function. Technical Report arXiv:1710.05941v2, Google Brain, 2018.
- [4] Joseph Redmon, Santosh Divvala, Ross Girshick, and Ali Farhadi. You Only Look Once: Unified, Real-Time Object Detection. 2015.
- [5] Alex Krizhevsky, Ilya Sutskever, and Geoffrey E Hinton. 1 ImageNet Classification with Deep Convolutional Neural Networks. *Advances In Neural Information Processing Systems*, 2012.
- [6] Kaiming He, Xiangyu Zhang, Shaoqing Ren, and Jian Sun. Deep Residual Learning for Image Recognition. Dec 2015.
- [7] Christian Szegedy, Wojciech Zaremba, Ilya Sutskever, Joan Bruna, Dumitru Erhan, Ian Goodfellow, and Rob Fergus. Intriguing properties of neural networks. Dec 2013.
- [8] M. Hein and M. Andriushchenko. Formal guarantees on the robustness of a classifier against adversarial manipulation. In I. Guyon, U. V. Luxburg, S. Bengio, H. Wallach, R. Fergus, S. Vishwanathan, and R. Garnett, editors, *Advances in Neural Information Processing Systems 30 (Proc. of the 31st NIPS)*, pages 2266–2276. Curran Associates, Inc., 2017.
- [9] L. Schott, J. Rauber, W. Brendel, and M. Bethge. Towards the first adversarially robust neural network model on mnist. *arXiv*, 2018.
- [10] E. Pekalska and R.P.W. Duin. *The Dissimilarity Representation for Pattern Recognition: Foundations and Applications*. World Scientific, 2006.
- [11] D. Nebel, M. Kaden, A. Bohnsack, and T. Villmann. Types of (dis-)similarities and adaptive mixtures thereof for improved classification learning. *Neurocomputing*, 268:42–54, 2017.
- [12] R.O. Duda and P.E. Hart. *Pattern Classification and Scene Analysis*. Wiley, New York, 1973.
- [13] C.M. Bishop. *Pattern Recognition and Machine Learning*. Springer Science+Business Media, LLC, New York, NY, 2006.
- [14] R.M. Gray. Vector quantization. *IEEE ASSP Magazine*, 1(2):4–29, 1984.
- [15] M. Biehl, B. Hammer, and T. Villmann. Prototype-based models in machine learning. *Wiley Interdisciplinary Reviews: Cognitive Science*, 7(2):92–111, 2016.

- [16] G. Voronoi. Nouvelles applications des parametres à la theorie des formes quadratiques. deuxième mémoire: Recherches sur les paralléloèdres primitifs. *J. reine angew. Math.*, 134:198–287, 1908.
- [17] P. L. Zador. Asymptotic quantization error of continuous signals and the quantization dimension. *IEEE Transaction on Information Theory*, IT-28:149–159, 1982.
- [18] E. Yair, K. Zeger, and A. Gersho. Competitive learning and soft competition for vector quantizer design. *IEEE Trans. on Signal Processing*, 40(2):294–309, February 1992.
- [19] Y. Linde, A. Buzo, and R.M. Gray. An algorithm for vector quantizer design. *IEEE Transactions on Communications*, 28:84–95, 1980.
- [20] S. P. Lloyd. Least squares quantization in PCM. *IEEE Transactions on Information Theory*, 28:129–137, 1982.
- [21] Teuvo Kohonen. *Self-Organizing Maps*, volume 30 of *Springer Series in Information Sciences*. Springer, Berlin, Heidelberg, 1995. (Second Extended Edition 1997).
- [22] D. Arthur and S. Vassilvitskii. k-means++: The advantages of careful seeding. In *Proceedings of the eighteenth annual ACM-SIAM symposium on Discrete algorithms, Philadelphia*, pages 1027–37. Society for Industrial and Applied Mathematics, 2007.
- [23] Thomas M. Martinetz, Stanislav G. Berkovich, and Klaus J. Schulten. 'Neural-gas' network for vector quantization and its application to time-series prediction. *IEEE Trans. on Neural Networks*, 4(4):558–569, 1993.
- [24] J.C. Bezdek. *Pattern Recognition with Fuzzy Objective Function Algorithms*. Plenum, New York, 1981.
- [25] R.J. Hathaway, J.W. Davenport, and J.C. Bezdek. Relational duals of the c-means clustering algorithms. *Pattern recognition*, 22(3):205–212, 1989.
- [26] N.R. Pal, K. Pal, J.M. Keller, and J.C. Bezdek. A possibilistic fuzzy c-means clustering algorithm. *IEEE Transactions on Fuzzy Systems*, 13(4):517–530, 2005.
- [27] R.J. Hathaway and J.C. Bezdek. NERF c-means: Non-Euclidean relational fuzzy clustering. *Pattern Recognition*, 27(3):429–437, 1994.
- [28] T. Villmann, S. Haase, and M. Kaden. Kernelized vector quantization in gradient-descent learning. *Neurocomputing*, 147:83–95, 2015.
- [29] T. Villmann and S. Haase. Divergence based vector quantization. *Neural Computation*, 23(5):1343–1392, 2011.
- [30] S. Miyamoto, H. Ichihashi, and K. Honda. *Algorithms for Fuzzy Clustering*, volume 229 of *Studies in Fuzziness and Soft Computing*. Springer, 2008.
- [31] Teuvo Kohonen. Learning Vector Quantization. *Neural Networks*, 1(Supplement 1):303, 1988.
- [32] A. Sato and K. Yamada. Generalized learning vector quantization. In D. S. Touretzky, M. C. Mozer, and M. E. Hasselmo, editors, *Advances in Neural Information Processing Systems 8. Proceedings of the 1995 Conference*, pages 423–9. MIT Press, Cambridge, MA, USA, 1996.
- [33] M. Kaden, M. Lange, D. Nebel, M. Riedel, T. Geweniger, and T. Villmann. Aspects in classification learning - Review of recent developments in Learning Vector Quantization. *Foundations of Computing and Decision Sciences*, 39(2):79–105, 2014.
- [34] S. Seo and K. Obermayer. Soft learning vector quantization. *Neural Computation*, 15:1589–1604, 2003.
- [35] S. Seo, M. Bode, and K. Obermayer. Soft nearest prototype classification. *IEEE Transaction on Neural Networks*, 14:390–398, 2003.

- [36] A. Villmann, M. Kaden, S. Saralajew, and T. Villmann. Probabilistic learning vector quantization with cross-entropy for probabilistic class assignments in classification learning. In L. Rutkowski, R. Scherer, M. Korytkowski, W. Pedrycz, R. Tadeusiewicz, and J.M. Zurada, editors, *Proceedings of the 17th International Conference on Artificial Intelligence and Soft Computing - ICAISC, Zakopane*, LNCS 10841, pages 736–749, Cham, 2018. Springer International Publishing, Switzerland.
- [37] E. Mwebaze, P. Schneider, F.-M. Schleif, J.R. Aduwo, J.A. Quinn, S. Haase, T. Villmann, and M. Biehl. Divergence based classification in learning vector quantization. *Neurocomputing*, 74(9):1429–1435, 2011.
- [38] M. Biehl, B. Hammer, and T. Villmann. Distance measures for prototype based classification. In L. Grandinetti, T. Lippert, and N. Petkov, editors, *Proceedings of the International Workshop on Brain-Inspired Computing 2013 (Cetraro/Italy)*, volume 8603 of LNCS, pages 100–116. Springer, 2014.
- [39] P. Schneider, B. Hammer, and M. Biehl. Distance learning in discriminative vector quantization. *Neural Computation*, 21:2942–2969, 2009.
- [40] P. Schneider, B. Hammer, and M. Biehl. Adaptive relevance matrices in learning vector quantization. *Neural Computation*, 21:3532–3561, 2009.
- [41] D. J. Willshaw and C. Von der Malsburg. How patterned neural connections can be set up by self-organization. *Proceedings of the Royal Society of London, Series B*, 194:431–445, 1976.
- [42] T. Heskes. Energy functions for self-organizing maps. In E. Oja and S. Kaski, editors, *Kohonen Maps*, pages 303–316. Elsevier, Amsterdam, 1999.
- [43] T. Villmann, S. Saralajew, A. Villmann, and M. Kaden. Learning vector quantization methods for interpretable classification learning and multilayer networks. In C. Sabourin, J.J. Merelo, A.L. Barranco, K. Madani, and K. Warwick, editors, *Proceedings of the 10th International Joint Conference on Computational Intelligence (IJCCI), Sevilla*, pages 15–21, Lissabon, Portugal, 2018. SCITEPRESS Science and Technology Publications, Lda. ISBN: 978-989-758-327-8.
- [44] L. Fischer, B. Hammer, and H. Wersing. Efficient rejection strategies for prototype-based classification. *Neurocomputing*, 169:334–342, 2015.
- [45] R. Herbei and M.H. Wegkamp. Classification with reject option. *The Canadian Journal of Statistics*, 34(4):709–721, 2006.
- [46] C.K. Chow. On optimum recognition error and reject tradeoff. *IEEE Transactions in Information Theory*, 16(1):41–46, 1970.
- [47] K. Urahama and Y. Furukawa. Gradient descent learning of nearest neighbor classifiers with outlier rejection. *Pattern Recognition*, 28(5):761–768, 1995.
- [48] A. Vailaya and A.K. Jain. Reject option for VQ-based Bayesian classification. In *International Conference on Pattern Recognition (ICPR)*, pages 2048–2051, 2000.
- [49] M. Yuan and M.H. Wegkamp. Classification methods with reject option based on convex risk minimization. *Journal of Machine Learning Research*, 11:111–130, 2010.
- [50] Alberto Munoz and Jorge Muruzabal. Self-organizing maps for outlier detection. *Neurocomputing*, 18(1):33–60, 1998.
- [51] Geoffrey E. Hinton, Nitish Srivastava, Alex Krizhevsky, Ilya Sutskever, and Ruslan R. Salakhutdinov. Improving neural networks by preventing co-adaptation of feature detectors. jul 2012.
- [52] Juergen Schmidhuber. Deep Learning in Neural Networks: An Overview. apr 2014.

- [53] H. deVries, R. Memisevic, and A. Courville. Deep learning vector quantization. In M. Verleysen, editor, *Proceedings of the European Symposium on Artificial Neural Networks, Computational Intelligence and Machine Learning (ESANN'2016)*, pages 503–508, Louvain-La-Neuve, Belgium, 2016. i6doc.com.
- [54] T. Villmann, M. Biehl, A. Villmann, and S. Saralajew. Fusion of deep learning architectures, multilayer feedforward networks and learning vector quantizers for deep classification learning. In *Proceedings of the 12th Workshop on Self-Organizing Maps and Learning Vector Quantization (WSOM2017+)*, pages 248–255. IEEE Press, 2017.
- [55] A. van den Oord, O. Vinyals, and K. Kavukcuoglu. Neural discrete representation learning. In I. Guyon, U.V. Luxburg, S. Bengio, H. Wallach, R. Fergus, S. Vishwanathan, and R. Garnett, editors, *Advances in Neural Information Processing Systems 30*, pages 6306–6315. Curran Associates, Inc., 2017.
- [56] E. Agustsson, F. Mentzer, M. Tschannen, L. Cavigelli, R. Timofte, L. Benini, and Luc V L. VanGool. Soft-to-hard vector quantization for end-to-end learning compressible representations. In I. Guyon, U.V. Luxburg, S. Bengio, H. Wallach, R. Fergus, S. Vishwanathan, and R. Garnett, editors, *Advances in Neural Information Processing Systems 30*, pages 1141–1151. Curran Associates, Inc., 2017.
- [57] H.-M. Yang, X.-Y. Zhang, F. Yin, and C.-L. Liu. Robust classification with convolutional prototype learning. In *Proceedings of the IEEE/CVF Conference on Computer Vision and Pattern Recognition, Salt Lake City*, pages 3474–3482. IEEE Press, 2018.
- [58] T. Villmann, S. Saralajew, J.R.D. John-Ravichandran, A. Villmann, and M. Kaden. *Recent Trends in Computational Intelligence and Machine Learning*, chapter Learning Vector Quantization Variants as Multilayer Networks for Interpretable Classification Learning, page in press. Springer, 2019.
- [59] Vincent Dumoulin and Francesco Visin. A guide to convolution arithmetic for deep learning. *arXiv preprint arXiv:1603.07285*, 2016.
- [60] K. Crammer, R. Gilad-Bachrach, A. Navot, and A. Tishby. Margin analysis of the LVQ algorithm. In S. Becker, S. Thrun, and K. Obermayer, editors, *Advances in Neural Information Processing (Proc. NIPS 2002)*, volume 15, pages 462–469, Cambridge, MA, 2003. MIT Press.
- [61] R. Hecht-Nielsen. Counterpropagation networks. *Appl. Opt.*, 26(23):4979–4984, December 1987.
- [62] Robert Hecht-Nielsen. Applications of counterpropagation networks. *Neural Networks*, 1(2):131–139, 1988.
- [63] D. Nebel, B. Hammer, K. Frohberg, and T. Villmann. Median variants of learning vector quantization for learning of dissimilarity data. *Neurocomputing*, 169:295–305, 2015.
- [64] B. Hammer, D. Nebel, M. Riedel, and T. Villmann. Generative versus discriminative prototype based classification. In T. Villmann, F.-M. Schleif, M. Kaden, and M. Lange, editors, *Advances in Self-Organizing Maps and Learning Vector Quantization: Proceedings of 10th International Workshop WSOM 2014, Mittweida*, volume 295 of *Advances in Intelligent Systems and Computing*, pages 123–132, Berlin, 2014. Springer.
- [65] K.L. Oehler and R.M. Gray. Combining image compressing and classification using vector quantization. *IEEE Transactions on Pattern Analysis and Machine Intelligence*, 17(5):461–473, 1995.
- [66] Chris Olah, Arvind Satyanarayan, Ian Johnson, Shan Carter, Ludwig Schubert, Katherine Ye, and Alexander Mordvintsev. The building blocks of interpretability. *Distill*, 2018. <https://distill.pub/2018/building-blocks>.
- [67] S. Saralajew, S. Nooka, M. Kaden, and T. Villmann. Learning vector quantization capsules. *Machine Learning Reports*, 12(MLR-02-2018):1–17, 2018. ISSN:1865-3960, http://www.techfak.uni-bielefeld.de/~fschleif/mlr/mlr_0_2017.pdf.

- [68] A. Athalye, N. Carlini, and D. Wagner. Obfuscated gradients give a false sense of security: Circumventing defenses to adversarial examples. In Jennifer Dy and Andreas Krause, editors, *Proceedings of the 35th International Conference on Machine Learning*, volume 80 of *Proceedings of Machine Learning Research*, pages 274–283. PMLR, 10–15 Jul 2018.
- [69] D.H. Wolpert. The lack of a priori distinctions between learning algorithms. *Neural Computation*, 8(7):1341–1390, 1996.
- [70] M. Biehl, A. Ghosh, and B. Hammer. Dynamics and generalization ability of LVQ algorithms. *Journal of Machine Learning Research*, 8:323–360, 2007.
- [71] A. Witoelar, M. Biehl, and B. Hammer. Equilibrium properties of offline LVQ. In M. Verleysen, editor, *Proc. Of European Symposium on Artificial Neural Networks (ESANN’2009)*, pages 535–540, Evere, Belgium, 2009. d-side publications.
- [72] T. Villmann, B. Hammer, F.-M. Schleif, T. Geweniger, T. Fischer, and M. Cottrell. Prototype based classification using information theoretic learning. In I. King, editor, *Proceedings of International Conference on Neural Information Processing (ICONIP), Hongkong 2006*, volume II, pages 40–49, Heidelberg, New York, 2006. Springer-Verlag.
- [73] J.C. Principe. *Information Theoretic Learning*. Springer, Heidelberg, 2010.
- [74] K. Torkkola. Feature extraction by non-parametric mutual information maximization. *Journal of Machine Learning Research*, 3:1415–1438, 2003.
- [75] Francesco Croce, Maksym Andriushchenko, and Matthias Hein. Provable robustness of relu networks via maximization of linear regions. *arXiv preprint arXiv:1810.07481*, 2018.
- [76] D.M.J. Tax and R.P.W. Duin. Growing a multi-class classifier with a reject option. *Pattern Recognition Letters*, 29:1565–1570, 2008.
- [77] T.C.W. Landgrebe, D. Tax, P. Pačlik, and R.P.W. Duin. The interaction between classification and reject performance for distance-based reject-option classifiers. *Pattern Recognition Letters*, 27:908–917, 2006.
- [78] P. L. Bartlett and M.H. Wegkamp. Classification with a reject option using a hinge loss. *Journal of Machine Learning Research*, 9:1823–1840, 2008.
- [79] C. deStefano, C. Sansone, and M. Vento. To reject or not to reject: That is the question - an answer in case of neural classifiers. *IEEE Transactions on Systems Man and Cybernetics - Part C: Applications and Reviews*, 30(1):84–94, 2000.
- [80] M.E. Hellman. The nearest neighbor classification rule with a reject option. *IEEE Transactions on Systems Science and Cybernetics*, 6:179–185, 1970.
- [81] T. Villmann, M. Kaden, A. Bohnsack, S. Saralajew, J.-M. Villmann, T. Drogies, and B. Hammer. Self-adjusting reject options in prototype based classification. In E. Merényi, M.J. Mendenhall, and P. O’Driscoll, editors, *Advances in Self-Organizing Maps and Learning Vector Quantization: Proceedings of 11th International Workshop WSOM 2016*, volume 428 of *Advances in Intelligent Systems and Computing*, pages 269–279, Berlin-Heidelberg, 2016. Springer.
- [82] T. Villmann, J.R.D. John-Ravichandran, S. Saralajew, and M. Biehl. Dropout in learning vector quantization networks for regularized learning and classification confidence estimation. *Machine Learning Reports*, 12(MLR-01-2018):5–6, 2018. ISSN:1865-3960, http://www.techfak.uni-bielefeld.de/~fschleif/mlr/mlr_0_2017.pdf.
- [83] P. Ramachandran, B. Zoph, and Q.V. Le. Searching for activation functions. Technical Report arXiv:1710.05941v1, Google Brain, 2018.
- [84] F. Lischke, T. Neumann, S. Hellbach, T. Villmann, and H.-J. Böhme. Direct incorporation of l_1 -regularization into generalized matrix learning vector quantization. In L. Rutkowski, R. Scherer, M. Korytkowski, W. Pedrycz, R. Tadeusiewicz, and J.M. Zurada, editors, *Proceedings of the 17th International Conference on Artificial Intelligence and Soft Computing - ICAISC, Zakopane, LNCS 10841*, pages 657–667, Cham, 2018. Springer International Publishing, Switzerland.

- [85] M. Strickert, B. Hammer, T. Villmann, and M. Biehl. Regularization and improved interpretation of linear data mappings and adaptive distance measures. In *Proc. of the WCCI Singapore 2013*, page in press. IEEE Computer Society Press, 2013.
- [86] P. Schneider, K. Bunte, H. Stiekema, B. Hammer, T. Villmann, and Michael Biehl. Regularization in matrix relevance learning. *IEEE Transactions on Neural Networks*, 21(5):831–840, 2010.
- [87] S. Sabour, N. Frosst, and G.E. Hinton. Dynamic routing between capsules. In I. Guyon, U. V. Luxburg, S. Bengio, H. Wallach, R. Fergus, S. Vishwanathan, and R. Garnett, editors, *Advances in Neural Information Processing Systems 30*, pages 3856–3866. Curran Associates, Inc., 2017.
- [88] A. Bohnsack, K. Domaschke, M. Lange, and T. Villmann. Learning matrix quantization and relevance learning based on Schatten- p -norms. *Neurocomputing*, 192:104 – 114, 2016.
- [89] S. Saralajew and T. Villmann. Adaptive tangent metrics in generalized learning vector quantization for transformation and distortion invariant classification learning. In *Proceedings of the International Joint Conference on Neural networks (IJCNN)*, Vancouver, pages 2672–2679. IEEE Computer Society Press, 2016.
- [90] S. Saralajew, D. Nebel, and T. Villmann. Adaptive Hausdorff distances and tangent distance adaptation for transformation invariant classification learning. In A. Hirose, editor, *Proceedings of the International Conference on Neural Information Processing (ICONIP)*, Kyoto, volume 9949 of *LNCS*, pages 362–371. Springer, 2016.
- [91] T. Nishida, S. Kurogi, and T. Saeki. An analysis of competitive and reinitialization learning for adaptive vector quantization. In *Proceedings of the International Joint Conference on Neural Networks*, volume 2, pages 978–983. Dept. of Control Engineering, Kyushu Institute of Technology, 2001.
- [92] A.K. Qin and P.N. Suganthan. Initialization insensitive LVQ algorithm based on cost-function adaptation. *Pattern Recognition*, 38:773–776, 2004.
- [93] H. L. Xiong, M. N. S. Swamy, and M. O. Ahmad. Competitive splitting for codebook initialization. *IEEE Signal Processing Letters*, 11(5):474–477, May 2004.
- [94] D.P. Kingma and J. Ba. Adam: A method for stochastic optimization. In *Proceedings of the International Conference on Learning Representations (ICLR), San Diego, 2015*, pages 1–13, 2015.